A Decision-Support Framework for Determining Minimum Synchronous Generation Requirements in Low-Inertia Isolated Power Systems

Phivos Therapontos, *Student Member, IEEE,* Christos Frangkeskou, *Member, IEEE*
Petros Aristidou, *Senior Member, IEEE*

***Abstract*—High renewable penetration in isolated power systems introduces stability and security challenges, primarily due to reduced synchronous inertia and limited fault-current contributions from inverter-based resources (IBRs). This paper presents a data-driven industrial decision-support framework that identifies secure unit commitment (UC) scenarios by integrating data analytics, generation clustering, scenario reduction, and multi-criteria security assessment. Historical measurements are processed, validated, and clustered to extract representative operating points. Candidate UC scenarios are then filtered through a six-stage procedure covering: (1) credible UC combinations; (2) frequency stability constraints; (3) minimum stable generation level; (4) fault level and system strength requirements; (5) static N-k contingency analysis; and (6) transient stability and low-voltage ride-through (LVRT) assessment via time-domain dynamic simulations. Compared to static or rule-based must-run practices, the framework provides transparent, explainable, and reproducible operational intelligence and quantifies trade-offs between security margins and renewable curtailment. A Cyprus transmission system case study shows that the proposed informatics-driven approach sharply reduces the feasible solution space and reveals dominant operational bottlenecks across operating conditions and prospective network developments, thereby supporting robust minimum synchronous generation requirements.**

***Index Terms*—Minimum synchronous generators, unit commitment, frequency stability, system strength, low-inertia power systems.**

I. Introduction

The global energy transition toward renewable energy sources (RES) has fundamentally transformed power system operation. As inverter-based resources (IBRs), including solar photovoltaic, and battery energy storage systems, increasingly displace conventional synchronous generators, power systems face unprecedented challenges in maintaining stability and security [1, 2]. Unlike synchronous machines, IBRs lack inherent inertia and contribute limited fault current during system disturbances, creating operational complexities that necessitate careful determination of must-run synchronous units [3].

The critical role of synchronous generators in providing system inertia cannot be overstated. These machines dampen frequency deviations following contingencies, enabling sufficient time for primary and secondary frequency response mechanisms to restore system balance [4]. Furthermore, voltage regulation becomes increasingly challenging in IBR-dominated systems, as these resources often require external reactive power support to maintain steady voltage profiles, particularly during grid faults or rapid load changes [5]. The reduced fault current contribution from IBRs also compromises protection system coordination, necessitating adequate synchronous capacity to maintain short-circuit levels required for reliable protection operation. In addition, lower fault levels reduce network strength and can increase the likelihood of voltage instability [6].

Operational complexities also arise from conflicting requirements: minimizing must-run units reduces RES curtailments, whereas insufficient synchronous capacity jeopardizes system stability. In Fig. 1 it can be seen that increasing the minimum synchronous generation requirements from 190 MW to 250 MW results in a significant increase in daily RES curtailments, from 408 MWh to 961 MWh.

Low-inertia isolated power systems, such as Cyprus, face amplified challenges due to their isolated nature and limited interconnection capabilities [7]. The Cyprus power system represents a paradigmatic case study for high-RES penetration scenarios, where conventional generation must be carefully balanced against renewable integration objectives while maintaining operational security under credible contingencies.

A. Literature Review and Contributions

Recent research has addressed various aspects of minimum synchronous generator requirements in low-inertia systems. Nakiganda et al. [8] proposed decomposition strategies for inertia-aware microgrid planning, while Pan et al. [9] investigated grid-forming converters for voltage stability in 100% renewable systems. However, these approaches typically focus on individual stability aspects rather than providing comprehensive frameworks that simultaneously address multiple technical constraints.

Across several power systems worldwide, system operators have imposed explicit measures to ensure sufficient rotational inertia and system strength as synchronous generation declines. The most direct approach involves minimum synchronous generator requirements, such as EirGrid and SONI the transmission system operators (TSOs) for Ireland and

P. Therapontos is with the University of Cyprus and the Electricity Authority of Cyprus (DSO), Nicosia, Cyprus (e-mail: ptherapo@eac.com.cy).
C. Fragkeskou is with the Transmission System Operator of Cyprus, Nicosia, Cyprus (e-mail: cfrangeskou@dsm.org.cy).
P. Aristidou is with the Cyprus University of Technology, Limassol, Cyprus (e-mail: petros.aristidou@cut.ac.cy).

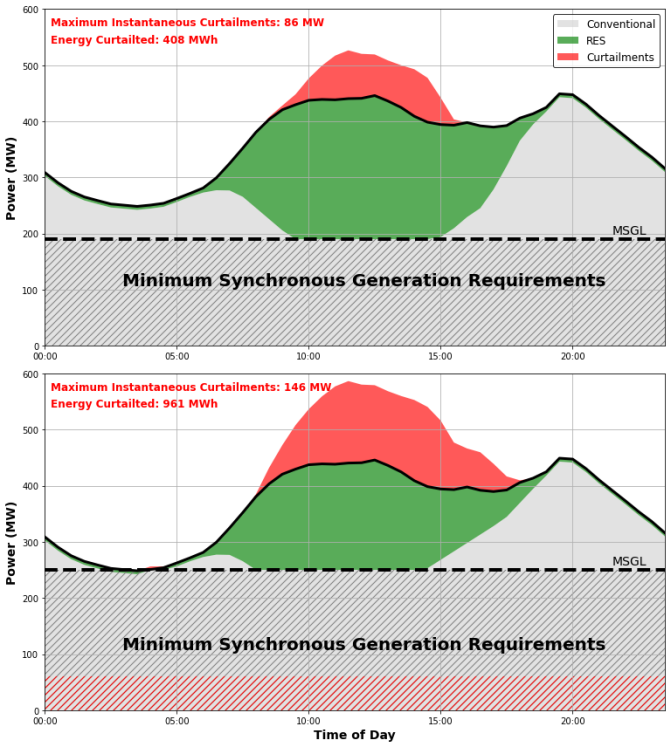

Fig. 1. Illustration of the trade-off between minimum synchronous generation requirements and RES curtailments.

Northern Ireland, which require at least four and three large fossil-fuelled units, respectively, to remain online under high renewable penetration [10]. The Australian Energy Market Operator (AEMO) in South Australia enforces a minimum of two large synchronous units along with synchronous condensers, to maintain stability [11]. Similarly, the Cypriot TSO (TSOC) requires four synchronous generators to be used as must-run units to prevent excessive rate of change of frequency (RoCoF) during generation outage events [12].

Other system operators define explicit minimum inertia thresholds. National Grid ESO in the UK has defined a minimum system floor of 120 GW·s [13]. The Electric Reliability Council of Texas (ERCOT) uses a dynamically calculated "critical inertia" threshold—typically around 88–100 GW·s. The threshold varies depending on the available fast frequency reserves [14, 15]. The small and islanded system of Hawaii has explicitly set a minimum rotating inertia level of 350 MW·s [16]. In contrast, many TSOs in Europe, Canada, and Nordic are not enforcing any inertia-related requirements [17–19].

The literature review indicates that most system operators have proposed minimum operating requirements, yet these are typically defined without accounting for critical factors such as system strength and maximum fault levels. Moreover, the practice of evaluating these minimum requirements on an annual basis presents significant limitations, as the actual requirements vary with real-time operating conditions. Consequently, this approach may lead to overestimations that result in unnecessary RES curtailments [7, 20]. These observations highlight the need for a robust and comprehensive decision-support framework that system operators can apply to determine minimum synchronous generation requirements while incorporating all essential operational characteristics of modern power systems.

The principal contributions of this work are:

- **A unified multi-stage decision-support framework for minimum synchronous generation requirements:** A six-stage filtering methodology that integrates RoCoF constraints, minimum stable generation level (MSGL), fault level and system strength checks, static N-k security, and low-voltage ride-through (LVRT) assessment to identify secure unit commitment (UC) scenarios.
- **A reproducible data analytics and scenario-reduction pipeline:** Automated processing, validation, and clustering of historical measurements to extract representative operating points and reduce the UC evaluation burden while preserving critical low-load conditions.
- **Industrial validation and actionable operational insights:** Demonstration on the Cyprus transmission system showing substantial reduction of the feasible UC solution space and identification of dominant bottlenecks and trade-offs relevant to renewable integration.

The remainder of this paper is organized as follows: Section II presents the mathematical formulation of the multi-stage filtering methodology; Section III describes the data processing; Section IV discusses implementation results; and Section V concludes with implications for power system operation.

II. Multi-Stage Filtering Methodology

The proposed methodology employs a systematic six-stage filtering process to determine acceptable UC scenarios for secure power system operation. Each stage addresses specific technical requirements, progressively refining the solution space while ensuring comprehensive coverage of operational constraints. A synopsis of the methodology is presented in Fig. 2.

The mathematical framework begins with the generation of all feasible UC combinations, followed by sequential application of stability and security filters. Let U denote the universe of all possible UC scenarios, and U_{si} represent the subset of acceptable scenarios after stage i. The filtering process ensures $U_{s6} \subseteq U_{s5} \subseteq \ldots \subseteq U_{s1} \subseteq U_{s0} = U$.

The final assessment is binary, and only the scenarios that satisfy all criteria are retained in U_{s6}. All UC combinations in U_{s6} ensure secure system operation under all credible contingencies. The system operator may therefore use appropriate market procedures to select the least-cost UC for must-run units. These market procedures may be conducted annually or even monthly or as determined by the system operator; however, the proposed methodology must be applied each time the procedure is performed. In the operational setting considered in this paper, the analysis is executed on a monthly basis to determine the must-run UC for the *next* month, using representative operating conditions derived from recent historical measurements.

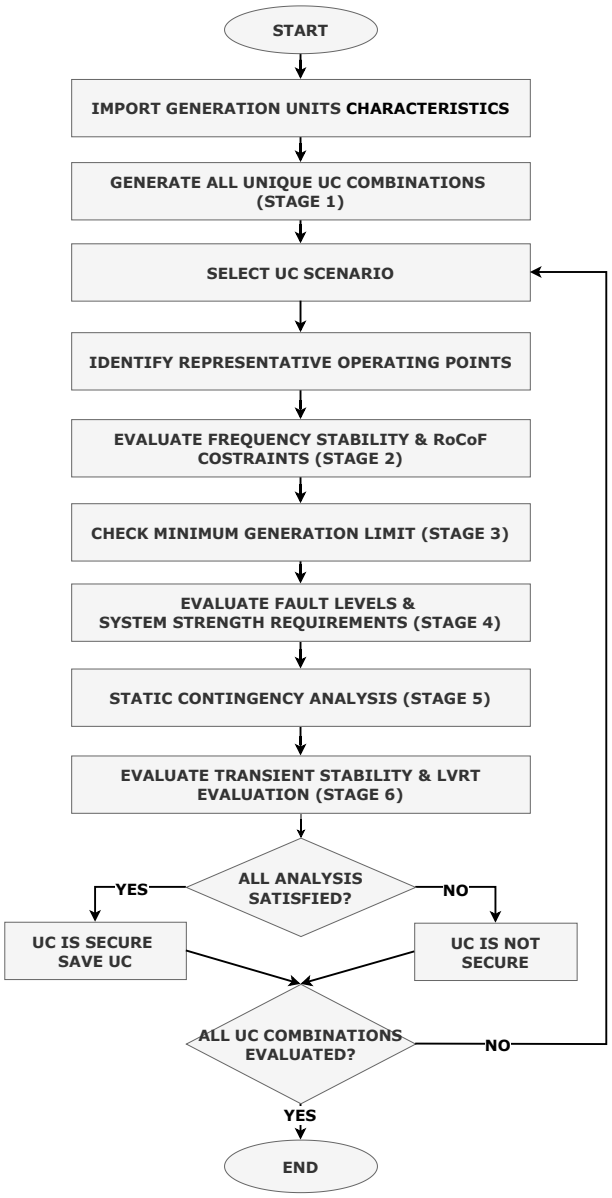

Fig. 2. Overview of the proposed multi-stage decision-support framework for filtering UC combinations based on security constraints.

A. Stage 1: Generation of Feasible UC Combinations

The initial stage enumerates all technically feasible generator combinations based on availability, maintenance schedules, and operational dependencies. To manage computational complexity, generators with similar technical characteristics are clustered using tolerance-based matching criteria.

Let G denote the set of all available synchronous generators, where each generator $g \in G$ is characterized by:

- Nominal capacity $S_{nom,g}$ (MVA)
- Maximum active power $P_{max,g}$ (MW)
- Minimum active power $P_{min,g}$ (MW)
- Inertia constant H_g (s)
- Equivalent reactance X_g (Ohm) at the point of common coupling (PCC)

Two generators g_i and g_j are considered identical if:

$$|S_{nom,g_i} - S_{nom,g_j}| \leq \text{TOL}_{\text{CAPACITY}} \quad (1)$$
$$|P_{max,g_i} - P_{max,g_j}| \leq \text{TOL}_{P_{max}} \quad (2)$$
$$|P_{min,g_i} - P_{min,g_j}| \leq \text{TOL}_{P_{min}} \quad (3)$$
$$|H_{g_i} - H_{g_j}| \leq \text{TOL}_{\text{INERTIA}} \quad (4)$$
$$|X_{g_i} - X_{g_j}| \leq \text{TOL}_{\text{IMPEDANCE}} \quad (5)$$

We note that, Equation 5, is used to verify that the two generators are located in the same power station. This is due to the fact that technically identical units installed on different power stations can have a different impact on the power system operation. Technical dependencies between generators, particularly for combined cycle gas turbine (CCGT) plants, are incorporated through constraint relationships described in Equation 6:

$$\text{Dependencies} = \{\text{Steam\_Unit} : [\text{Gas\_Unit\_1}, \text{Gas\_Unit\_2}]\} \quad (6)$$

Therefore, the Steam Unit of a CCGT can be activated only if at least one of the Gas Units is activated.

B. Stage 2: Frequency Stability and RoCoF Constraints

The methodology for evaluating frequency stability involves two critical contingency scenarios: maximum outage loss (non-inertial) and largest synchronous unit loss (with inertia).

For contingencies involving units without rotational inertia (e.g., high-voltage direct current (HVDC) links), RoCoF is computed as:

$$\text{RoCoF}_1 = \left| \frac{-P_{\text{loss,max}} \cdot f_N}{2 \cdot E_{\text{kin,total}}} \right| \leq \text{RoCoF}_{\text{MAX}} \quad (7)$$

where $P_{loss,max}$ (MW) represents the maximum credible non-inertial loss, f_N (Hz) is the nominal system frequency, $E_{kin,total} = \sum_{g \in G}(u_g H_g S_{g,N})$ is the total kinetic energy of committed units, and $RoCoF_{MAX}$ is the maximum allowed value of RoCoF defined by the TSO. For the loss of the largest committed synchronous generator:

$$\text{RoCoF}_2 = \left| \frac{-P_{\text{loss,unit}} \cdot f_N}{2 \cdot (E_{\text{kin,total}} - E_{\text{loss,unit}})} \right| \leq \text{RoCoF}_{\text{MAX}} \quad (8)$$

where $P_{loss,unit}$ is the maximum active power of the tripped generator, and $E_{loss,unit} = H_{trip} \cdot S_{trip}$ represents the kinetic energy contributed by the disconnected unit. The minimum required kinetic energy is determined as:

$$E_{kin}^{req} \leq \sum_{g \in G} (u_g H_g S_{g,N}) + \sum_{sc \in SCs} (u_{sc} H_{sc} S_{sc,N}) + \sum_{vi \in VI} (u_{vi} H_{vi} S_{vi,N}) \quad (9)$$

where $u_g \in \{0, 1\}$ is the binary commitment variable for generator g. SCs denotes the set of synchronous condensers and VI denotes the set of virtual inertia providers (e.g., grid-forming IBRs) that can provide kinetic energy. Moreover, H_{sc}

and H_{vi} are the corresponding inertia constants. Scenarios violating $RoCoF_{MAX}$ are eliminated:

$$U_{s2} = \{u \in U_{s1} : \text{viol\_cont}(u) = 0\} \tag{10}$$

C. Stage 3: Minimum Stable Generation Level

The third stage ensures that committed units can operate feasibly under minimum net load demand conditions. Let U_{s2} denote the set of RoCoF-compliant scenarios. For each scenario $u \in U_{s2}$, the total MSGL is:

$$P_{MSGL}(u) = \sum_{g \in G} (u_g \cdot P_{min,g}) \tag{11}$$

The minimum net load for the analysis period is defined as:

$$P_{load}^{min} = \min_t \{P_{net}(t)\} \tag{12}$$

Acceptable commitments must satisfy:

$$P_{MSGL}(u) \leq P_{load}^{min} - R^{\downarrow} \tag{13}$$

where $R^{\downarrow}$ represents the downward spinning reserve requirement. Scenarios violating the MSGL limit are eliminated:

$$U_{s3} = \{u \in U_{s2} : \text{viol\_cont}(u) = 0\} \tag{14}$$

D. Stage 4: Fault Levels and System Strength Requirements

1) Fault Levels: It is important to verify that prospective fault levels are below the interrupting capability of the equipment. Hence, for each UC scenario, the IEC 60909 method [21] is used to compute three-phase fault currents $I_{kss,i}$ at each high-voltage (HV) busbar i. The corresponding short-circuit capacity (SCC) is:

$$\text{SCC}_i = \frac{|V_{th,i}|^2}{|Z_{th,i}|} \tag{15}$$

where $V_{th,i}$ and $Z_{th,i}$ are the Thévenin equivalent voltage and impedance at busbar i. Scenarios are rejected if any busbar exceeds voltage-dependent limits:

$$I_{kss,i} > I_{kss,limit}(U_k, \text{bus } i) \tag{16}$$

2) System Strength: In this analysis, the Short Circuit Ratio (SCR), which is a well-known indicator of power system strength, is used to assess system strength [22]. The SCR at each transmission substation j is computed as:

$$\text{SCR}_j = \frac{\text{SCC}_j}{P_{IBR,j}} \tag{17}$$

where SCC_j is the minimum short-circuit capacity among substation busbars, and $P_{IBR,j}$ represents aggregated IBRs capacity. System strength adequacy requires:

$$\text{SCR}_j \geq \text{SCR}_{min} \tag{18}$$

where typical thresholds are: SCR > 3 (strong grid), $1 <$ SCR < 3 (weak grid requiring mitigation), and SCR < 1 (very weak grid unstable without external support).

Scenarios violating either maximum fault current or system strength limits are eliminated:

$$U_{s4} = \{u \in U_{s3} : \text{viol\_cont}(u) = 0\} \tag{19}$$

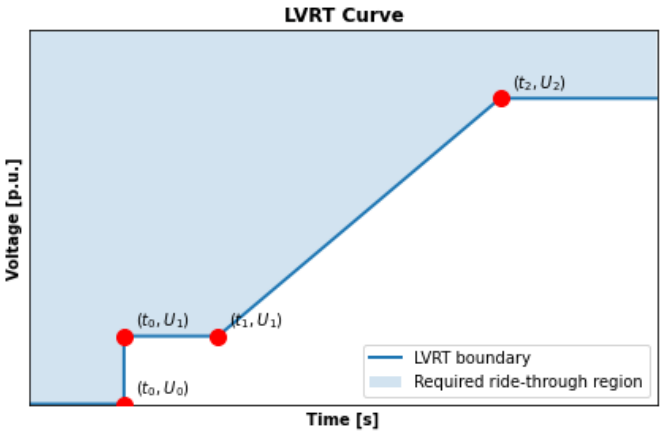

Fig. 3. Generic LVRT envelope used for compliance assessment (minimum admissible voltage versus time).

E. Stage 5: Static N-k Contingency Analysis

Static N-k security assessment verifies system performance under k element outages. The analysis considers line, transformer, and generator contingencies while evaluating voltage security and thermal loading constraints. The mathematical formulation involves solving AC power flow equations under contingency conditions:

$$P_i^c = V_i^c \sum_{j=1}^{n} V_j^c (G_{ij}^c \cos\theta_{ij}^c + B_{ij}^c \sin\theta_{ij}^c) \tag{20}$$

$$Q_i^c = V_i^c \sum_{j=1}^{n} V_j^c (G_{ij}^c \sin\theta_{ij}^c - B_{ij}^c \cos\theta_{ij}^c) \tag{21}$$

where superscript c denotes contingency conditions, and G_{ij}^c, B_{ij}^c represent modified admittance matrix elements. Security constraints include:

$$V_i^{min} \leq V_i^c \leq V_i^{max}, \quad \forall i \in N, \forall c \in C \tag{22}$$

$$|I_{ij}^c| \leq I_{ij}^{max}, \quad \forall (i,j) \in L^c, \forall c \in C \tag{23}$$

where N represents the set of all buses, C denotes selected contingencies, and L^c indicates transmission elements under contingency c. Scenarios violating security criteria are eliminated:

$$U_{s5} = \{u \in U_{s4} : \text{viol\_cont}(u) = 0\} \tag{24}$$

F. Stage 6: Transient Stability and LVRT Assessment

The final stage employs root-mean-square (RMS) dynamic simulations to verify transient stability and LVRT compliance. Critical fault scenarios are defined with three-phase short circuits at selected busbars, cleared after CCT_{actual}. The CCT_{actual} time (ms) can be calculated using the reformulated transient stability margin η as:

$$\text{CCT}_{\text{actual}} = (1 + \eta)\, \text{CCT}_{\text{critical}} \tag{25}$$

A typical LVRT curve is presented in Figure 3. LVRT compliance verification employs piecewise linear curves specifying minimum acceptable voltage levels. Compliance requires:

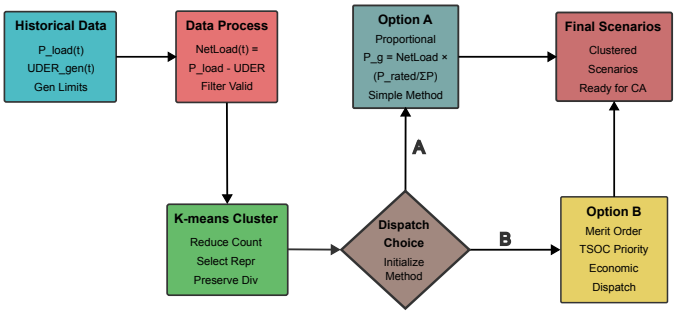

Fig. 4. Data analytics workflow for scenario generation: validation, preprocessing, clustering, and extraction of representative operating points from historical measurements.

$$V(t_i) - V_{LVRT,interp}(t_i) \geq 0, \quad \forall t_i \tag{26}$$

Scenarios violating the LVRT requirement are eliminated:

$$U_{s6} = \{u \in U_{s5} : \text{viol\_cont}(u) = 0\} \tag{27}$$

III. Data Analytics Pipeline

The proposed framework leverages historical operational measurements to construct a compact yet representative set of operating points for subsequent security assessment. This workflow is implemented using the *TSOC Data Analysis*[1] tool developed by the Sustainable Power Systems Lab (SPS-L), which provides a reproducible Python API and command-line interface for data ingestion, validation, and representative operating point extraction from TSO datasets. In practice, month-based filtering is employed to enable efficient processing of large time-series archives; if the operator targets a specific planning horizon (e.g., a given month), then the pipeline isolates the relevant records and ensures consistent feature construction across all subsequent stages. Accordingly, each monthly run produces a set of representative operating points and a vetted set of secure UC combinations that support next-month must-run scheduling decisions.

A specialized data analysis platform processes time-series data including:

- Substation active and reactive power measurements
- Generator voltage setpoints and reactive power output
- Wind farm generation profiles
- Shunt element reactive power and tap positions

From these measurements, the pipeline derives a set of standardized indicators that are used throughout the paper. In particular, it computes system-wide load quantities (total load and net load), summarizes renewable penetration levels, and produces descriptive statistics and profiles that allow the analyst to contextualize representative points before running security studies. Moreover, the tool supports generator categorization (e.g., voltage-control versus PQ-control behavior) and reactive power calculations, which are essential when voltage-sensitive constraints (e.g., LVRT) are evaluated downstream.

[1]Source code: https://github.com/SPS-L/TSOC-data-analysis. Documentation: https://tsoc-data-analysis.sps-lab.org/.

As illustrated in Fig. 4, data processing follows a multi-level validation framework. First, **basic validation** performs data type verification, operational bounds checking, missing data interpolation (gap filling), and unit-consistency checks. Next, **enhanced validation** applies outlier detection, data continuity verification, cross-parameter validation, and integrity logging, so that suspicious records are traceable and corrections are auditable. Finally, **preprocessing** performs statistical outlier removal, zero-variance feature elimination, correlation analysis, and feature engineering to capture load diversity and renewable penetration indicators. In other words, the pipeline aims to remove artifacts without suppressing genuine operational variability, since the latter determines the diversity of credible operating conditions.

After validation, the pipeline executes a structured workflow that can be summarized as follows:

1) **Ingest and harmonize**: read the operational datasets (e.g., Excel-based archives), standardize naming and units, and align time stamps.
2) **Compute derived quantities**: calculate total load and net load, aggregate wind generation profiles, and compute reactive power indicators that support subsequent voltage-security analyses.
3) **Categorize controllable resources**: identify generator operating modes (voltage-control versus PQ-control) and record setpoints relevant to steady-state and dynamic studies.
4) **Validate and log**: apply basic and enhanced validation checks and generate integrity logs that document corrections, exclusions, and remaining anomalies.
5) **Extract representative operating points**: perform clustering and export representative points together with diagnostics and visualizations.

Representative operating point generation uses a two-tier clustering approach consistent with the tool documentation. **Standard clustering** applies K-means with automatic cluster selection (k = 2 to 10) and is evaluated using the Silhouette Score, Calinski–Harabasz Index, and Davies–Bouldin Index. This stage is optimized for practical use on large archives, and it explicitly retains critical low-load points near minimum active power generation limits, since these operating conditions are the most restrictive for the minimum stable generation filter in Stage 3. On the other hand, **enhanced clustering** is triggered when standard clustering yields poor quality (typically Silhouette < 0.4). In that case, the pipeline introduces dimensionality reduction via Principal Component Analysis and considers alternative clustering algorithms (DBSCAN, hierarchical clustering, Gaussian Mixture Models), selecting the best-performing option based on clustering diagnostics.

From an implementation standpoint, the tool exposes a high-level workflow that supports both scripted studies and repeatable operational use. A typical execution parses the raw spreadsheets, applies validation, and generates cleaned datasets and summary tables. Next, representative points are extracted together with diagnostics that document the selected number of clusters, clustering quality indices, and preprocessing details. Crucially, the extraction is parameterized so that system-

specific limits can be enforced consistently (for example, maximum power ranges and minimum-active-generation-related thresholds), thereby ensuring that edge operating conditions remain visible to the subsequent UC filtering stages rather than being averaged out by clustering.

The tool also supports structured configuration, which improves traceability and facilitates sensitivity studies. Configuration areas cover the system description, data-file mapping, validation settings (types, bounds, and gap-filling rules), representative operating point settings (cluster limits and quality thresholds), enhanced clustering options (alternative algorithms and preprocessing toggles), and visualization settings (automatic generation of plots and summary figures). On the other hand, if input data quality is degraded or metadata are incomplete, then the pipeline's comprehensive logging and error handling provide a pragmatic troubleshooting layer: anomalies are flagged, corrective actions are documented, and the analyst can reproduce the full processing chain without manual intervention.

Quality thresholds guide clustering selection:

- Excellent (Silhouette > 0.7): Standard clustering
- Good (0.5-0.7): Enhanced method consideration
- Acceptable (0.25-0.5): Enhanced clustering application
- Poor (< 0.25): Advanced preprocessing and algorithms

The pipeline exports both data products and diagnostics. Data products include cleaned time-series tables, representative operating point tables, and summary statistics for load and renewable generation (profiles and distributions). Diagnostics include clustering quality metrics, selected algorithm parameters, and comprehensive logs that facilitate troubleshooting and reproducibility; when enhanced clustering is used, the diagnostics also document the selected algorithm and dimensionality-reduction steps. Consequently, the resulting representative operating points and associated diagnostics are used as inputs to the downstream unit commitment filtering stages, thereby enabling transparent, repeatable, and computationally tractable security assessment across diverse operating conditions.

IV. Results

The proposed methodology was implemented and validated using the Cyprus transmission system model in DIgSILENT PowerFactory [23]. The system parameters used in the analysis are based on the Cypriot Grid Code Requirements [24]:

- Maximum allowable RoCoF: 1 Hz/s
- Upward spinning reserve ($R^{\uparrow}$): 40 MW
- Downward spinning reserve ($R^{\downarrow}$): 25 MW
- Critical clearing time $CCT_{critical}$: 120 ms
- Transient stability margin (η): 0.25
- Minimum SCR threshold: 3.0
- Transmission Substation Switchgear Rating: 31.5 kA
- LVRT curve:
  - U_0 = 0 p.u, t_0 = 0.2 s
  - U_1 = 0.15 p.u, t_1 = 0.2 s
  - U_2 = 0.9 p.u, t_2 = 3 s

A. Stage 1 - Unique and Feasible UC Combinations

The power system of Cyprus currently has 25 synchronous generator units. Internal combustion engines and small Gas Turbines are neglected since they are not being used as base load units. From the remaining 15 generation units, four groups of generator units have been identified as "unique" based on the criteria of Equations (1-5). As a result, the following groups have been developed:

- Group 1: Steam Turbines 60MW (6 units)
- Group 2: Steam Turbines 120MW (3 units)
- Group 3: Gas Turbines 72.5MW (part of CCGT) (4 units)
- Group 4: Steam Turbines 75MW (part of CCGT) (2 units)

The total number of possible UC combinations is $2^{15} = 32,768$. By applying the generation grouping, this number is reduced to 419 combinations. When the dependency limit for CCGT units (Equation 6) is enforced, the set of valid UC combinations further decreases to U_{s1} = 335.

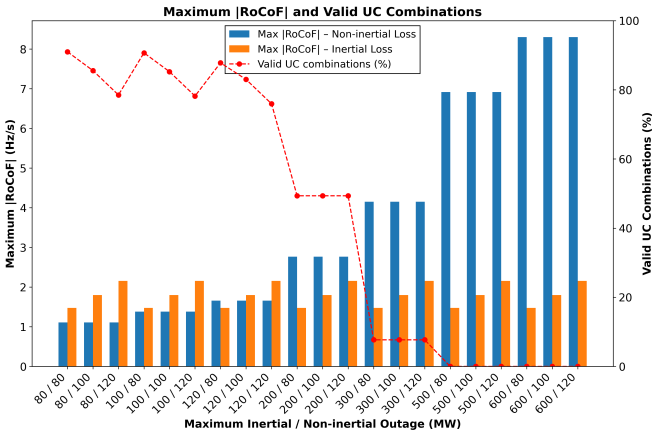

Fig. 5. Stage 2 results: maximum rate of change of frequency (RoCoF, Hz/s) and percentage of UC combinations satisfying RoCoF constraints versus the assumed maximum credible outage (MW).

B. Stage 2 - RoCoF Constraints

The second stage of the analysis addresses frequency stability based on RoCoF constraints. The proposed methodology evaluates both inertial and non-inertial outage scenarios.

1) Impact of Generation Outage: The results presented in Fig. 5 show that when the maximum outage loss remains below 120 MW, the disconnection of a must-run unit yields higher RoCoF values than an equivalent non-inertial loss. However, for larger non-inertial outages, RoCoF values rise sharply. Concurrently, the percentage of valid UC combinations after the Stage 2 drops from approximately 80% to 50%, effectively halving the number of feasible UC combinations. These results confirm that the proposed methodology can also support system planning applications. Specifically, the analysis reveals that the system can tolerate up to a 300 MW non-inertial loss, beyond which the percentage UC combinations fall extremely low.

2) Impact of Virtual Inertial and Synchronous Condensers: In this analysis, the impact of virtual inertia provided by grid-forming IBRs or by the installation of synchronous condensers is evaluated. These resources effectively reduce the kinetic energy requirements imposed on synchronous generation units, as expressed in Equation (9). Fig. 6 shows the percentage

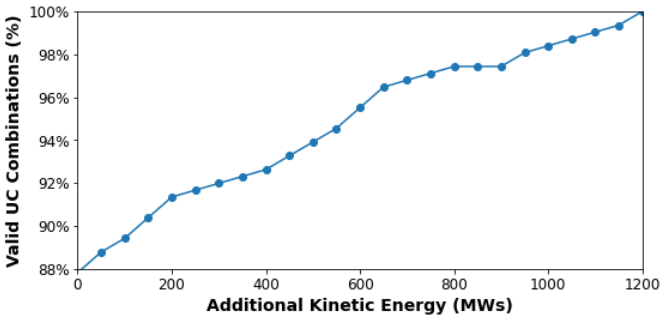

Fig. 6. Stage 2 sensitivity: percentage of UC combinations satisfying RoCoF constraints versus additional kinetic energy (MW·s) provided by synchronous condensers and/or virtual inertia.

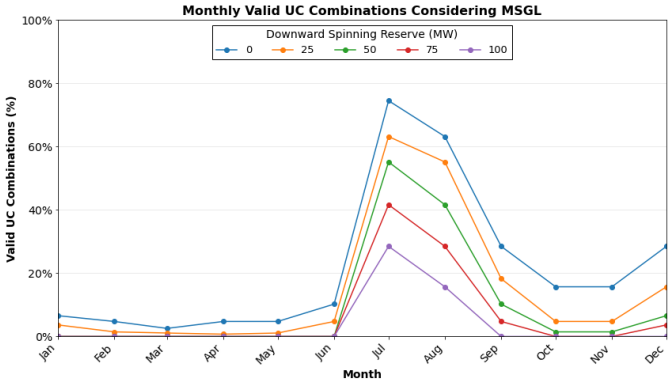

Fig. 7. Stage 3 results: monthly percentage of UC combinations satisfying the MSGL constraint under the specified downward reserve requirement.

of valid UC combinations as a function of the additional kinetic energy (MWs) supplied by these resources. It can be observed that an additional 1200 MWs is required to render all UC combinations feasible. This relationship highlights the scalability of the proposed methodology, which can be employed to assess future system needs and to evaluate the impact of prospective developments in the power system.

C. Stage 3 - Minimum Stable Generation Level

Furthermore, the influence of the MSGL filter on the number of feasible UC combinations after Stage 2 (U_{s2}) was evaluated. This assessment included a sensitivity analysis in which the downward spinning reserve requirement ($R^{\downarrow}$) was varied. The parameter $R^{\downarrow}$ enables the system operator to account for potential decreases in load demand and/or increases in RES generation.

Figure 7 illustrates that the percentage of valid UC combinations varies substantially across different months. This variation is driven by the strong seasonal dependence of system load demand [7]. During the summer months, higher load levels enable UC configurations with a larger number of committed units to satisfy the MSGL constraint. In contrast, during the autumn and spring months—when cooling and heating requirements are minimal—the percentage of valid UC combinations remains consistently below 20%. Additionally, $R^{\downarrow}$ has a significant impact on the number of feasible combinations, as it effectively reduces the net system load.

D. Stage 4 - Fault Levels and System Strength Analysis

1) Fault Levels: Moreover, the fault levels of the network have been evaluated for the UC combinations that satisfy RoCoF and MSGL constraints (U_{s3}) for November. The results for each UC combination and each transmission substation are presented in the heatmap of Fig. 8. The substations are sorted on the x-axis based on their I_{kss} values (kA). In this manner, the proximity of transmission substations is explicitly taken into account in the analysis. It is evident that for different UC combinations, the SCC differ across substations. As expected, neighboring substations exhibit SCC of similar magnitude. Furthermore, some substations exhibit a significant change of I_{kss} depending on the UC; specifically, some substations experience an increase in I_{kss} of more than 40%. This

TABLE I
STAGE 4 CASE STUDY: SUMMARY OF THE UC3 AND UC10 COMMITMENTS USED FOR SYSTEM STRENGTH COMPARISON (UNITS COMMITTED PER POWER STATION, MSGL, AND MAXIMUM ROCOF).

Characteristic	UC 3	UC 10
Committed Generators at VPS	4	2
Committed Generators at DPS	0	2
MSGL (MW)	180	174
Maximum RoCoF (Hz/s)	-0.95	-0.89

demonstrates that, when evaluating minimum synchronous requirements, it is important to consider fault levels, as these can vary significantly depending on the UC. It can also be observed that the resulting fault currents remain well below the equipment's withstand capability. This is mainly attributed to the reduced number of synchronous generation units in all 13 UC combinations, which is a consequence of satisfying the MSGL filter in Stage 3.

2) System Strength: This analysis evaluates and compares the impact of two UC combinations (UC3 and UC10) that satisfy both RoCoF and MSGL constraints on system strength. The main characteristics of the two combinations are summarized in Table I. The two UC combinations have the same number of committed generator units and similar MSGL and RoCoF. The results of the analysis are presented in Fig. 9. Compared to UC3, UC10 exhibits increased SCR values in the Dekhelia Power Station (DPS) area (red-shaded region), while a reduction of up to 20% is observed in the Vasilikos Power Station (VPS) area (purple-shaded region). This outcome was expected, as two synchronous generators originally located in VPS are decommissioned and committed in DPS under UC10. This finding highlights that the proposed methodology considers also geospatial characteristics, which are critical for system strength assessment. We note that no SCR violations have been identified in the present analysis.

E. Stage 5 - Static N-1 Contingency Analysis

Stage 5 involved an N-1 static contingency analysis (while Stage 5 generally accommodates N-k, an N-1 formulation is considered here for clarity). The outaged elements included transmission lines and power transformers. In all simulated scenarios, the security constraints defined by Equations (22)

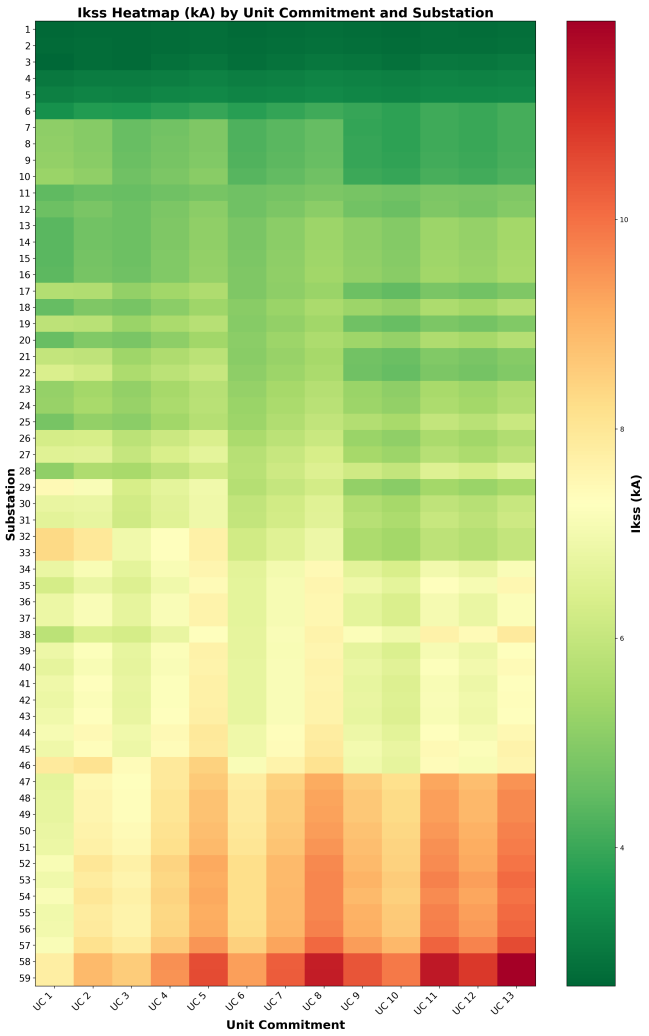

Fig. 8. Stage 4 results: heatmap of three-phase initial short-circuit current (I_{kss}, kA) at HV busbars across transmission substations for each UC combination.

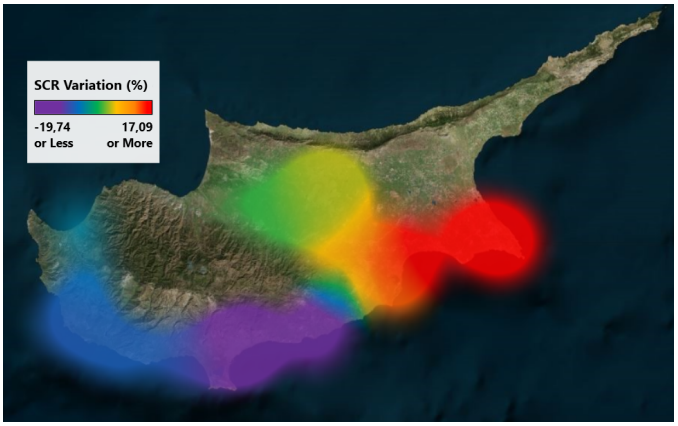

Fig. 9. Stage 4 results: spatial variation of SCR for UC10 relative to UC3.

and (23) were satisfied. This outcome is attributed to the relatively low overall system load demand during the examined period.

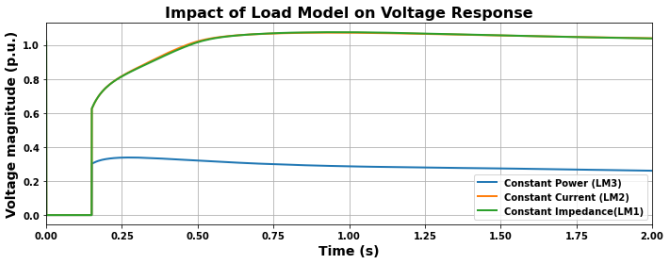

Fig. 10. Stage 6 results: impact of load model (ZIP representation) on post-fault voltage recovery in RMS simulations.

TABLE II
STAGE 6: ZIP LOAD MODEL COEFFICIENTS FOR ACTIVE AND REACTIVE POWER AND THE CORRESPONDING PERCENTAGE OF UC COMBINATIONS SATISFYING THE LVRT CRITERION.

Load Model	Active Power			Reactive Power			Valid UC Combinations
	a	b	c	a	b	c	
1	1	0	0	1	0	0	100%
2	0	1	0	0	1	0	100%
3	0	0	1	0	0	1	31%
4	0	1	0	1	0	0	92%
5	0.1	0.2	0.7	0.1	0.2	0.7	38%
6	0.3	0.3	0.4	0.3	0.3	0.4	53%

F. Stage 6 - Transient Stability and LVRT Assessment

In the last analysis, an LVRT assessment is performed. An RMS analysis for a three-phase fault with zero impedance at HV busbars is simulated for each UC and each representative operating point. Emphasis is given on the impact of load modeling on LVRT assessment. The active and reactive power of each load can be calculated using Equation (28) [25]. This equation represents the well-known impedance-current-power (ZIP) model. The values of a, b, c are the relative participation of constant load impedance, constant current, and constant power, respectively.

$$p, q = p_0, q_0 \left[a \left(\frac{u}{u_0} \right)^2 + b \left(\frac{u}{u_0} \right) + (1 - a - b) \right] \quad (28)$$

From Fig. 10 it is evident that load modeling has a significant impact on the LVRT assessment. For Load Models (LM) 1 and 2, where the active and reactive power are modeled as constant impedance and currents respectively, voltage recovers fast within LVRT limits. This behavior is attributed to the fact that both active and reactive power decrease as functions of the voltage magnitude. In contrast, under LM 3, where both active and reactive power are modeled as constant power the voltage fails to recover above 0.4 p.u. Table II summarizes the percentage of UC combinations that satisfy the LVRT requirement for different load models. For LM 1 and LM 2 all UC combinations successfully satisfy the LVRT requirements. On the other hand 69% of the UC combinations fail to meet the LVRT criteria for LM 3. For LM 4, LM 5, and LM 6, the results are more restrictive than those obtained with LM 1 and LM 2, but less restrictive than LM 3. Based on [25, 26], LM 4—where active power is modeled as constant power and reactive power as constant impedance—is recommended when detailed load data are unavailable.

TABLE III
DOMINANT OPERATIONAL CONSTRAINTS UNDER REPRESENTATIVE OPERATING CONDITIONS AND THEIR PRIMARY DRIVERS.

Condition	Constraint	Cause
Low load demand	MSGL	Reduced net load
Peak load demand	RoCoF	Increased inertial loss
High RES capacity	System strength	SCR reduction
New HVDC link	RoCoF	Increased non-inertial loss
New Power Station	Fault level	Higher SCC

G. Constraint Dominance and Operational Bottlenecks

Based on the results of the analysis, 12 UC combinations can be used to verify the secure operation of the system under the examined contingencies for November. MSGL is the primary limiting constraint having only 5% of valid UC combinations, followed by the RoCoF limit with 88%. Other constraints currently have minimal impact on secure UC combinations. However, future developments or variation in the operating conditions can elevate the impact of these factors. Table III summarizes the dominant operational constraints identified by the proposed methodology under representative system evolution and operating scenarios. Specifically, the development of the planned new power station is expected to increase fault levels. Consequently, UC combinations with a large number of synchronous generation units concentrated in the same region may no longer be valid from a fault-level perspective. At the same time, the projected increase in the installed IBRs capacity may lead to potential SCR violations, particularly in remote areas where fault levels have already been reduced.

V. DISCUSSION

A. Methodological Advantages

The proposed decision-support framework is designed for an operational reality in which minimum synchronous generation requirements are not a static policy parameter, but an outcome that depends on operating conditions, credible contingencies, and technology mix. Accordingly, its primary advantage is that it evaluates these interdependencies explicitly, rather than relying on isolated criteria or fixed must-run heuristics.

First, the framework provides **comprehensive coverage** by combining frequency stability, minimum stable generation level (MSGL), fault level, system strength, static security, and time-domain dynamic checks within a single workflow. Next, it provides a **transparent process**: the stage-by-stage filtering reveals *why* UC combinations fail, which constraints bind, and how the feasible set contracts as additional security requirements are enforced. Moreover, it supports **practical implementation** because each stage maps to standard studies already used in utility environments (e.g., short-circuit calculations, power-flow contingency analysis, and RMS simulations) and can be executed within established tools such as PowerFactory. Finally, the approach remains **scalable and adaptable**. If the system operator needs broader coverage, then additional constraints or alternative services (e.g., virtual inertia and synchronous condensers, as reflected in the kinetic-energy formulation) can be incorporated consistently. On the other hand, if the study scope must be reduced, then selected stages can be simplified while preserving the same transparent decision logic.

B. Computational Burden

The computational burden is primarily driven by the number of available synchronous generator units, since the underlying UC search space grows combinatorially. Although Stage 1 substantially reduces this space through grouping and feasibility screening, the proposed approach will generally become impractical for large-scale power systems with hundreds of conventional units. In the Cyprus implementation, typical execution times range from approximately 3 to 40 hours on a conventional computer, depending on the number of available generators and the number of valid UC combinations remaining after Stage 3 (MSGL).

Importantly, the framework is intended for offline, medium-term operation. In the operational setting considered here, the full analysis is executed **once per month** to support next-month must-run UC selection; therefore, it does not compete with real-time dispatch timelines, and it can be scheduled as a periodic planning task. Nevertheless, if runtime must be reduced, then the study scope can be tailored in a technically consistent manner. For example, the LVRT assessment can be omitted, and the contingency set in Stage 5 (or the fault set in Stage 6) can be limited to the most critical elements, thereby reducing dynamic simulations while maintaining a conservative screening philosophy. In other words, the framework trades computational intensity for decision transparency; however, it also allows the operator to explicitly select this trade-off, rather than making it implicitly through ad-hoc simplifications.

C. Accuracy and Limitations

As demonstrated in the LVRT case study, load modeling can materially affect transient responses and, consequently, feasibility outcomes. Input assumptions also matter. If the maximum credible outage is underestimated (either for inertial or non-inertial loss), then the methodology may overstate feasibility; conversely, conservative outage assumptions will shrink the feasible set and may increase must-run requirements. In the same way, reserve settings, protection limits, and system strength thresholds introduce modeling choices that are often system-specific; if these parameters change, then the feasible UC set must be recomputed.

Uncertainty further limits the strength of deterministic conclusions. On the data side, operational measurements may contain missing values, time-alignment errors, sensor bias, or non-stationarities; even with validation and clustering, these effects can distort representative operating points, particularly near low-load conditions that drive the MSGL filter. On the modelling side, parameter uncertainty (e.g., inertia constants, governor responses, load model coefficients, and converter control settings) and structural uncertainty (e.g., aggregated load representations and simplified protection behaviour) can shift stability margins and change which constraints become binding. Future work will therefore focus on quantifying the

impact of these uncertainties through targeted sensitivity studies and, where appropriate, uncertainty-aware (probabilistic) evaluations for the most influential parameters and scenarios.

Moreover, the screening power is bounded by the contingency set. Static and dynamic stages can only assess the contingencies that are explicitly modelled; hence, omissions (or overly narrow selection) may leave relevant weaknesses undetected, whereas an overly broad set may impose unnecessary conservatism and computational cost. Finally, the methodology inherits the limitations of the underlying simulation abstractions. For example, RMS studies provide a practical representation for many utility workflows; however, if converter-dominated dynamics, protection interactions, or fast control phenomena are dominant, then higher-fidelity modelling and targeted EMT-style studies may be required for final validation.

For these reasons, future work will also consider systematic model-validation procedures, structured parameter-sweep studies (e.g., outage sizes, reserve settings, load models, and contingency definitions), and update strategies that maintain consistency as the generation portfolio, network topology, and protection constraints evolve.

VI. Conclusions

This paper presents a comprehensive decision-support framework for determining minimum synchronous generator requirements tailored for low-inertia isolated power systems. The approach successfully integrates multiple technical constraints—frequency stability, system strength, static security, and transient stability—within a unified framework suitable for practical utility applications.

Key findings include:

1) The six-stage filtering process provides a systematic and transparent assessment of UC combinations, ensuring a comprehensive coverage of operational security requirements.
2) Generator clustering techniques effectively reduce computational complexity while maintaining essential technical diversity for stability analysis.
3) Representative operating point clustering enables comprehensive assessment across diverse system conditions while maintaining computational tractability.
4) Sequential constraint application reveals the relative importance of different stability limitations.
5) The methodology successfully balances renewable energy utilization objectives with stringent security requirements, providing quantitative justification for must-run unit decisions.

The Cyprus transmission system implementation demonstrates the framework's practical applicability and effectiveness in addressing real-world power system challenges. The approach provides TSOs with robust decision-support capabilities for medium-term unit commitment planning, ensuring secure grid operation during the transition to IBR-dominated power systems.

As power systems worldwide navigate similar renewable integration challenges, the proposed methodology offers a structured approach to balancing environmental objectives with reliability requirements. The framework's modularity and comprehensive constraint coverage make it readily adaptable to different system characteristics.

References

[1] R. W. Kenyon, V. N. Sewdien, Y. Wang, M. H. Donovan, and S. Chowdhury, "Stability and control of power systems with high penetrations of inverter-based resources: An accessible review of current knowledge and open questions," *Solar Energy*, vol. 210, pp. 149–168, 2020.

[2] NERC, "Inverter-based resource performance issues report," Tech. Rep., 2023.

[3] I. M. Dudurych, "The impact of renewables on operational security," *IEEE Power & Energy Magazine*, pp. 37–45, Feb. 2021.

[4] ENTSO-E, "Frequency stability evaluation criteria for the synchronous zone of continental Europe - Requirements and impacting factors," Tech. Rep., 2016.

[5] S. Atakan, H. Gangammanavar, and S. Sen, "Operations planning experiments for power systems with high renewable resources," *Optimization Online*, April 2020.

[6] M. O. Qays, I. Ahmad, D. Habibi, A. Aziz, and T. Mahmoud, "System strength shortfall challenges for renewable energy-based power systems: A review," *Renewable and Sustainable Energy Reviews*, 2023.

[7] P. Therapontos, R. Tapakis, P. Aristidou, and A. Charalambides, "RES Curtailments in Cyprus: A Review of Technical Constraints and Solutions," *Solar Energy Advances*, p. 100097, 2025.

[8] A. M. Nakiganda, S. Dehghan, and P. Aristidou, "A decomposition strategy for inertia-aware microgrid planning models," *IET Generation, Transmission & Distribution*, December 2024.

[9] D. Pan, X. Wang, F. Liu, and R. Shi, "Transient stability of voltage-source converters with grid-forming control: A design-oriented study," *IEEE Journal of Emerging and Selected Topics in Power Electronics*, vol. 8, no. 2, pp. 1019–1033, 2020.

[10] EirGrid and SONI, "Potential Solutions for Mitigating Technical Challenges Arising from High RES-E Penetration on the Island of Ireland," Tech. Rep., 2021.

[11] F. Arraño-Vargas, Z. Shen, S. Jiang, and et al., "Challenges and mitigation measures in power systems with high share of renewables—the Australian experience," *Energies*, 2022.

[12] P. Therapontos, R. Tapakis, A. Nikolaidis, and P. Aristidou, "Increasing RES Penetration in the Cyprus Power System: Current and Future Challenges," in *MEDPOWER2022*, 2022.

[13] National Grid ESO, "Frequency Risk and Control Report (FRCR) 2023–2024," London, UK, Tech. Rep., Dec. 2023.

[14] Electric Reliability Council of Texas, "Inertia: Basic Concepts and Impacts on the ERCOT Grid," Austin, TX, USA, Tech. Rep., Apr. 2018.

[15] ——, "Role of fast frequency response in lowering the minimum inertia requirement," in *DOE Grid Stability Workshop*, Texas, USA, Nov. 2024.

[16] "Hawai'i island near-term grid needs assessment – stage 3," Hawaiian Electric Company (HECO), Hawai'i, USA, Tech. Rep., Jul. 2021.

[17] Fingrid / Svenska kraftnät / Statnett / Energinet, "Requirement for minimum inertia in the nordic power system," Nordic Transmission System Operators, Tech. Rep., Aug. 2023.

[18] ENTSO-E, "Inertia and rate of change of frequency (rocof)," Brussels, Belgium, Tech. Rep., Dec. 2020.

[19] A. Boričić, S. Frohn, S. Liu, and J. Bos, "Inertia in the dutch power grid: Trends and implications," *Cigre science and engineering*, vol. CSE038, 2025.

[20] EirGrid and SONI, "Annal Renewable Energy Constraint and Curtailment Report 2024," 2024.

[21] *IEC 60909-0: Short-circuit currents in three-phase a.c. systems – Part 0: Calculation of currents*, IEC Std., 2016.

[22] CIGRE Working Group B4.62, "Connection of wind farms to weak ac networks," CIGRE, Paris, France, Tech. Rep. WG B4.62, 2014.

[23] "PowerFactory 2023 - User Manual," *DIgSILENT GmbH.*, 2023.

[24] TSOC, "Transmission rules - version 1.1.0," Tech. Rep., October 2024.

[25] CIGRÉ Working Group C4.605, "Modelling and aggregation of loads in flexible power networks," CIGRÉ, Technical Brochure 566, 2014.

[26] *IEEE Guide for Load Modeling and Simulation for Power Systems*, IEEE Power & Energy Society Std. IEEE Std 1547.7-2013, 2013.